

## Numerical simulation of airflow over two successive tunnel greenhouses

J.N. Dados, V.P. Fragos\*, G.K. Ntinis, S. Papoutsis-Psychoudaki, and Ch. Nikita-Martzopoulou

Department of Hydraulics, Soil Sciences and Agricultural Engineering, Aristotle University of Thessaloniki,  
GR-54124 Thessaloniki, Greece

Received December 2, 2010; accepted January 20, 2011

**A b s t r a c t.** This paper shows the airflow over two successive, single span tunnel greenhouses into a wind tunnel. The governing Navier-Stokes and continuity equations are solved numerically, using the Galerkin finite element method. The Reynolds number is calculated according to the height of the structures and the inlet free stream velocity and its values are varied from 0.02 to 1 200. The airflow is viscous, incompressible, steady and nominated to be two-dimensional, while the greenhouses are extended to the whole width of the tunnel. Computed values, for the stream-wise and cross-wise velocity and pressure, are derived by the solution of the mathematical model, at all points of the computational flow field. The analysis of the results provided numerical predictions, such as streamlines in the flow field, vortices around the structures, distributions of stream-wise velocity and separation-reattachment lengths of the boundary layer. The numerical procedure is validated by the results of other researchers.

**K e y w o r d s:** greenhouse, two-dimensional viscous flow, Navier-Stokes equations, finite elements

### INTRODUCTION

Wind is one of the most important factors to be taken into account for the construction of agricultural, urban or industrial buildings. The geometry of agricultural structures affects the airflow and subsequently the distribution of wind loads. Wind affects load distribution patterns on structures but also influences various design parameters with respect to structural, environmental and energy aspects. Greenhouses are usually light structures, thus wind loads may result in the destruction or deterioration of their components. Wind can also transfer and accumulate air, water, dust and snow influencing the operation of heating and ventilation systems. For all these reasons, experimental, theoretical and computational study of airflow is required around and over greenhouse structures, in full scale or into wind tunnel conditions

(Bournet and Boulard, 2010; Molina-Aiz *et al.*, 2010; Norton *et al.*, 2007). The main advantage of the wind tunnel is the control of airflow characteristics, thus large number of studies includes experimental and numerical results into wind tunnels (Erpul *et al.*, 2000; Hwang *et al.*, 1999; Nalbandi *et al.*, 2010; Psychoudaki *et al.*, 2005 a,b).

The viscous, incompressible, steady, two-dimensional flow, over different types of structures, has been examined by many researchers. Macagno and Hung (1967) approached experimentally, the flow in a conduit expansion. Acrivos *et al.* (1968) conducted experimental studies in a wide range of structures and fluids. Denham and Patric (1974) studied experimentally the flow over a backward-facing step. Armaly *et al.* (1983) examined the flow over a backward-facing step in a wind tunnel, for  $70 \leq Re \leq 8\,000$ . Antoniou and Bergeles (1988) studied the effect of the structure geometry in the recirculation region, downstream of a mounted obstacle in a wind tunnel.

Many researchers have suggested numerical solutions of the mathematical models which are describing the viscous, steady, two-dimensional flow (Navier-Stokes and continuity equations). For this purpose, they used different mathematical models in order to simulate the above equations and different numerical methods to solve them. Macagno and Hung (1967) used the finite differences method to solve the Navier-Stokes and continuity equations. Leone and Gresho (1981) simulated the steady flow over a backward-facing step solving the Navier-Stokes equations with the finite element method. Hong *et al.* (1991) transformed the Navier-Stokes and continuity equations in function-vorticity equations and solved them with the alternating directions implicit method (ADI). Fragos *et al.* (1997) simulated the laminar, isothermal, incompressible, two-dimensional flow,

\*Corresponding author's e-mail: fragos@agro.auth.gr

at steady state, over a rectangular mounted obstacle, solving the Navier-Stokes equations with the Galerkin finite element method. Vassiliou *et al.* (1998) used the finite differences method to solve the Reynolds equations in order to simulate the airflow outside and inside a double span tunnel greenhouse. Boum *et al.* (1999) simulated the laminar, two-dimensional flow, at steady state, around a surface mounted obstacle, solving the Navier-Stokes equations with the finite volume method. Psychoudaki *et al.* (2005a,b) studied numerically the airflow over a single span tunnel greenhouse in a wind tunnel, using the Galerkin finite element method.

This paper deals with the numerical simulation of the airflow over two successive, single span tunnel greenhouses, using the Navier-Stokes and continuity equations. The boundary conditions are placed so as to satisfy the flow conditions over two successive tunnel greenhouses, into a wind-tunnel.

The purpose of this research is to simulate the steady mass transfer in the particular walls.

MATERIALS AND METHODS

The dimensionless Navier-Stokes and continuity Eqs (1) and (2), respectively, are used to solve the two-dimensional, viscous, incompressible, steady flow over two successive greenhouses in a wind tunnel:

$$u\nabla u = -\nabla p + \frac{1}{\text{Re}} \nabla^2 u, \tag{1}$$

$$\nabla u = 0, \tag{2}$$

where:  $u=(u^*,v^*)$  is the velocity vector of the fluid with  $u^*$  and  $v^*$  its components in the x and y directions, respectively,  $p$  is the pressure and Re is the Reynolds number.

The governing equations have been rendered dimensionless by using the following characteristic magnitudes ( $h, V, P_o, \text{Re}$ ), where:  $h$  is the height of the greenhouse (m),  $V$  is the uniform approaching velocity of the fluid (inlet free stream velocity,  $\text{m s}^{-1}$ ),  $P_o = \rho V^2$  is the pressure intensity ( $\text{N m}^{-2}$ ),  $\rho$  is the density of the fluid ( $\text{N s}^2 \text{m}^{-4}$ ),  $\text{Re}=Vh/\nu$  is the Reynolds number with respect to the height of the greenhouse,  $h$ , and  $\nu$  is the kinematic viscosity of the fluid ( $\text{m}^2 \text{s}^{-1}$ ).

The present work studies the two-dimensional flow over two successive tunnel greenhouses at different Reynolds numbers, from 0.02 to 1 200. The design parameters of each prototype greenhouse are: height ( $h=3.6$  m), width ( $w=6.8$  m) and length ( $l=16$  m) (Vassiliou *et al.*, 1998). The scale prototype greenhouse-mathematical model is 1:16. The computational domain is shown in Fig. 1.

A uniform free stream flow is used as boundary condition at the entrance of the computational domain. The no-slip boundary conditions are imposed along the walls of the wind tunnel and the greenhouse structures. The outlet boundary condition is a free boundary condition that permits the fluid to leave the computational domain freely without any distortion (Fragos *et al.*, 2007; Malamataris, 1991; Papanastasiou *et al.*, 1992).

The Standard Galerkin finite element method was used in order to solve the governing Eqs (1) and (2) along with the appropriate initial and boundary conditions (Gresho and Sani, 1998; Owen and Hinton, 1980; Zienkiewicz *et al.*, 2000). The finite element code was written in the programming language VISUAL FORTRAN 90/95. The computational mesh in the flow field and the detailed mesh around the greenhouse structures are shown in Fig. 2.

The pressure is formulated by a linear basis function, while the velocity by a quadratic one. The unknown velocities and pressure are expanded in Galerkin basis functions.

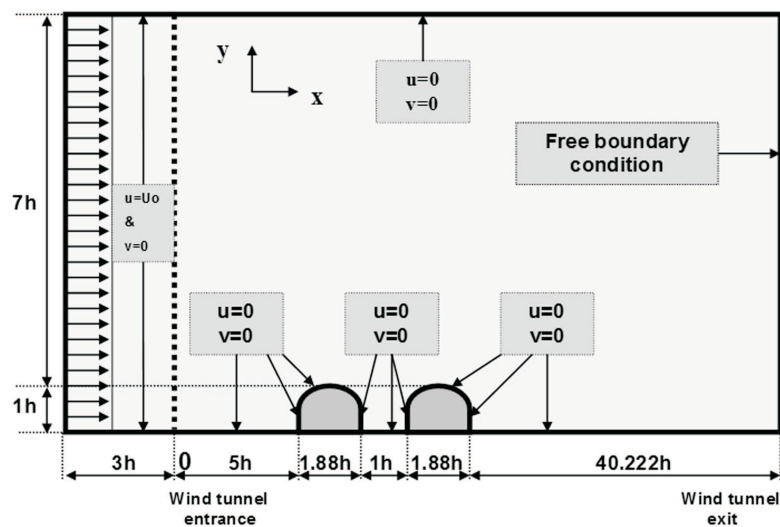


Fig. 1. Computational domain of nominally two-dimensional flow over two successive greenhouse structures.

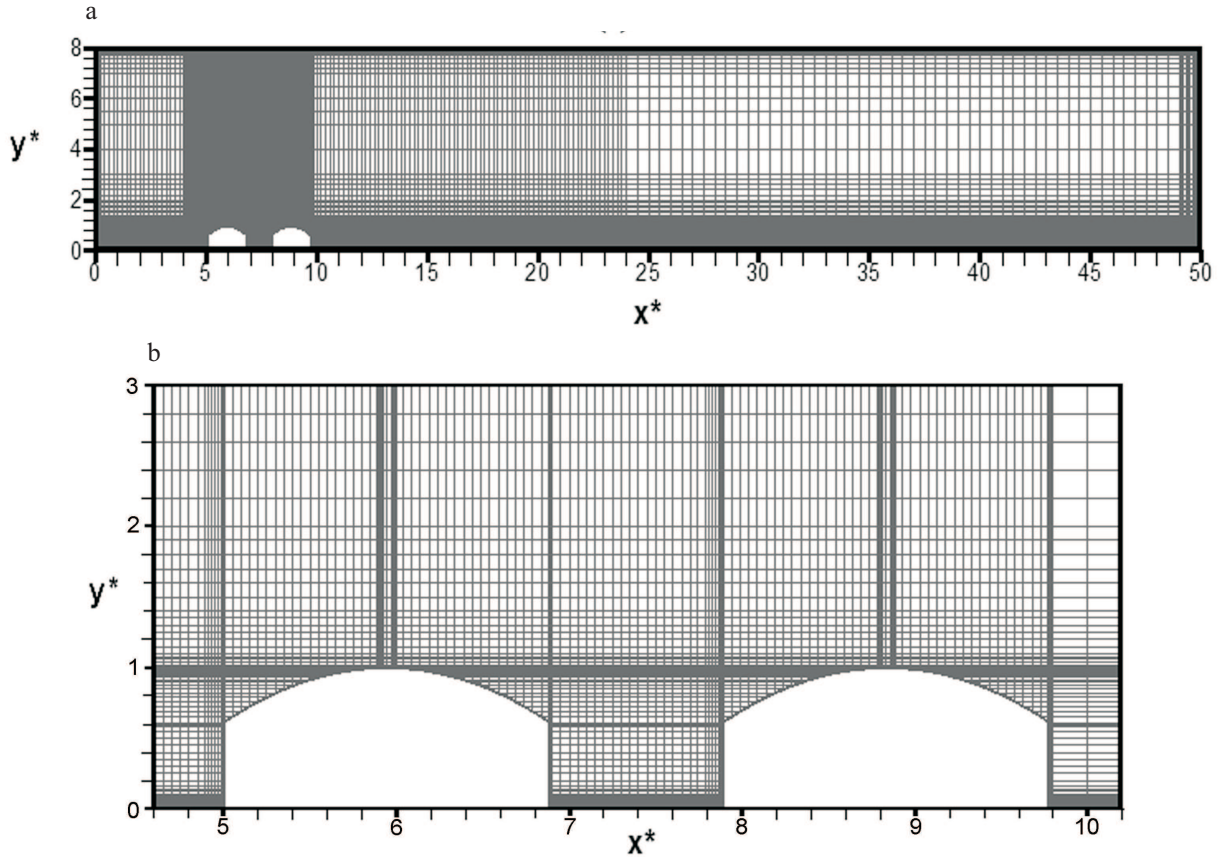


Fig. 2. Computational mesh of present work (a), details mesh around two successive greenhouses (b).

Equations (1) and (2) are weighted integrally with the basis functions. By applying the divergence theorem, the weighted residuals ( $R_c^i, R_M^i$ ) become:

$$R_c^i = \int_V \nabla u \Psi^i dV, \tag{3}$$

$$R_M^i = \int_V \left[ u \nabla u - \nabla \left( -pI + \frac{1}{Re} T \right) \right] \Phi^i dV - \int_S \left[ -pI + \frac{1}{Re} T \right] \Phi^i dS, \tag{4}$$

where:  $I$  is the identity matrix,  $T = \nabla u + (\nabla u)^T$  is the stress tensor of the Newtonian fluid and  $\Psi^i, \Phi^i$  are the linear and quadratic basic functions in Eqs (3) and (4), respectively. The non linear system of Eqs (3) and (4) is solved numerically with the Newton-Raphson method.

The flow domain is tessellated in 24 824 finite elements with 100 031 nodes. At each node of the finite elements, the unknown variables of the stream-wise ( $u^*$ ) and the cross-wise ( $v^*$ ) velocities are numerically calculated. Also, the

pressure is calculated at the edge nodes of the finite elements. The resulting linear system consists of 225 302 unknowns. Each Reynolds number step needs three iterations to converge quadratically. The maximum error of the Newton-Raphson method is  $10^{-6}$  for velocities and  $5 \cdot 10^{-4}$  for pressure calculations. Each iteration uses 2.81 CPU minutes, on a computer desktop (Intel Core 2 Duo E4600 2.40 GHZ and 2GB RAM). Details of the computational mesh and the flow characteristics are shown in Table 1.

RESULTS AND DISCUSSION

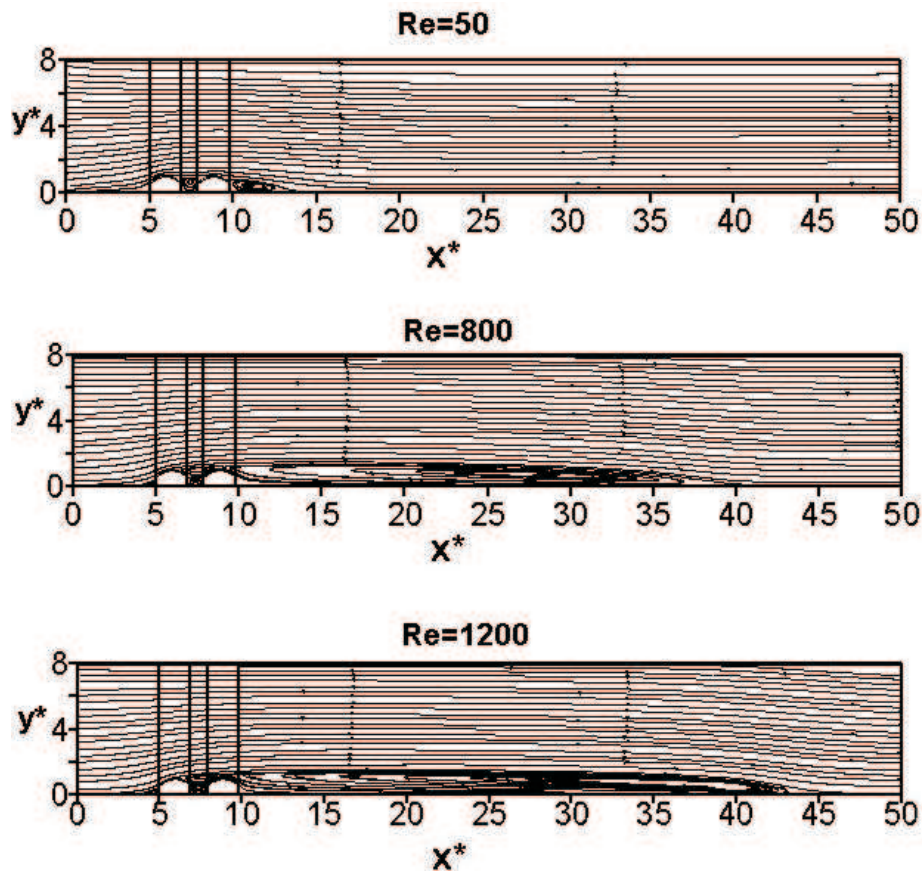
The streamlines along the computational domain ( $L^*=50$ ), is presented in Fig. 3, for selected Reynolds numbers ( $50 \leq Re \leq 1200$ ). Three recirculation regions of airflow are observed at the streamlines distributions, the first one upstream of the 1st greenhouse, the second one between the successive greenhouses and the third one downstream of the 2nd greenhouse. The particular geometry of these greenhouses causes the boundary layer separation which leads to the formation of the recirculation regions. It should be noted that the recirculation flow length is increasing as the Reynolds number is increasing, downstream of the 2nd greenhouse.

**Table 1.** Data of computational mesh

Parameters	Values
Dimensionless height of wind tunnel (H)	8
Dimensionless length of wind tunnel (L)	50
Reynolds Numbers	0.02-1 200
Number of elements (NE)	24 824
Number of nodes (NH)	100 031
Number of unknowns (NP)	225 302
CPU time per iteration	2.81 min
Computer used	Intel Core 2 Duo E4600 2.40 GHZ 2GB RAM
Location of first greenhouse	$5 \leq x \leq 6.888$
Location of second greenhouse	$7.888 \leq x \leq 9.776$
Height of greenhouse	$0 \leq y \leq 1$

Details of the streamlines upstream of the first greenhouse and distributions of the stream-wise velocity ( $u^*$ ) for different Reynolds numbers ( $50 \leq Re \leq 1\ 200$ ) are presented in Fig. 4. The separation of the flow takes place just before the vertical side edge of the first greenhouse. The separation point of the airflow is moving away from the edge. The formed vortex is growing in size as the Reynolds number is increasing, in the upstream end of the first greenhouse. The velocity distribution is uniform,  $u^* = 1$ , at the entrance and almost to the total height of the wind tunnel. Negative values of stream-wise velocity are observed in the vicinity of the upstream side of the first greenhouse, in the recirculation region.

Figure 5 shows details of the streamlines over two successive greenhouses and the development of the boundary layer at the stream-wise velocity ( $u^*$ ) profiles, regarding to the wind tunnel height, for  $50 \leq Re \leq 1\ 200$ . It is observed that the computed streamlines, from the reattachment point ( $x^* = 5$ ) and beyond, smoothly surround both of the greenhouses roofs. Another separation point is appeared over the roof, which is more obvious as the Reynolds number is increasing. For  $Re \geq 200$ , it is observed that the separation of flow starts at the middle of the first greenhouse and it is

**Fig. 3.** Streamlines of the flow for Reynolds numbers: 50, 800 and 1 200.

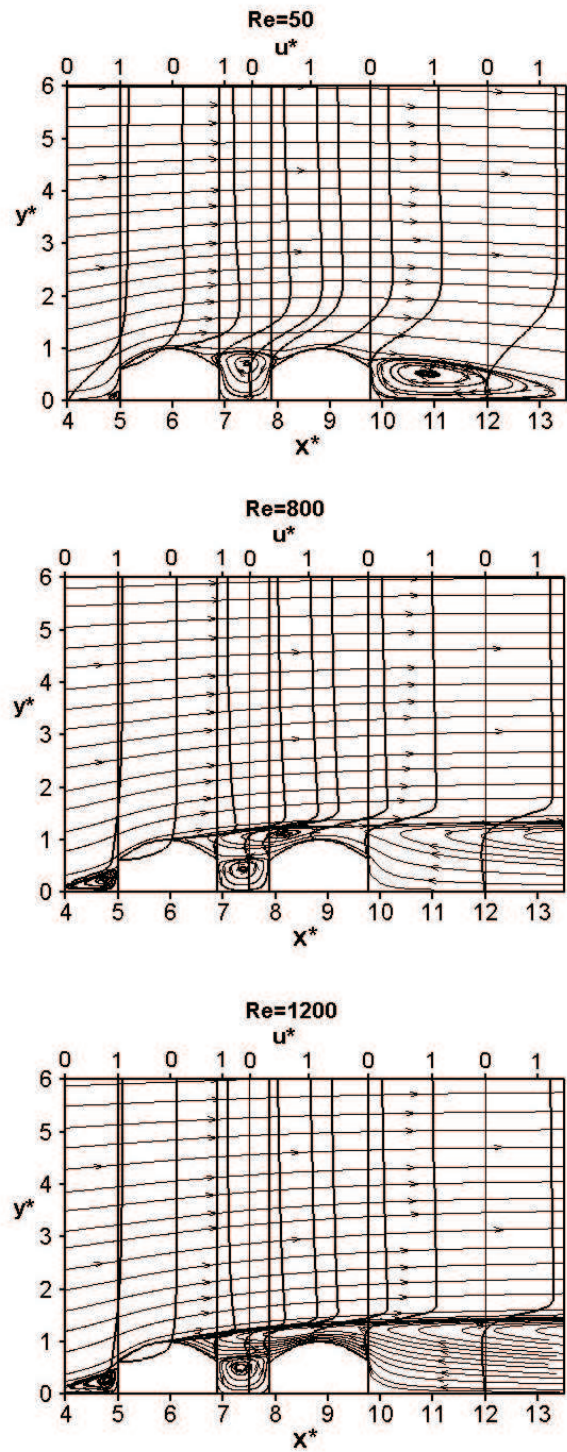
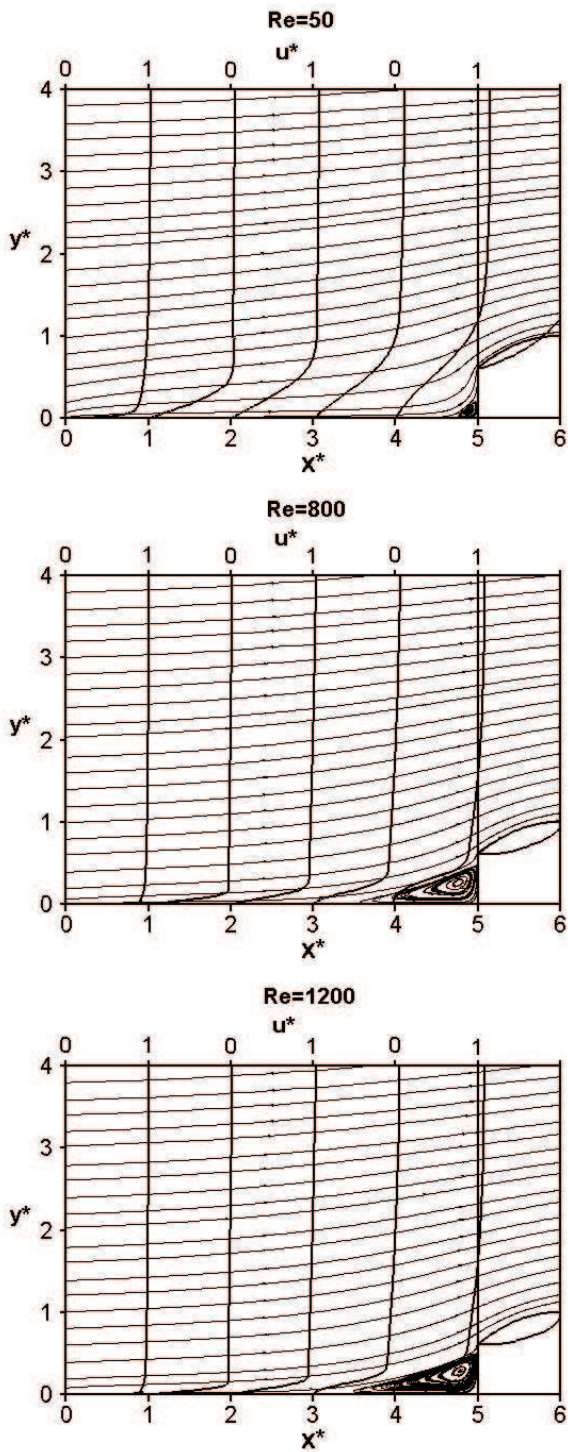


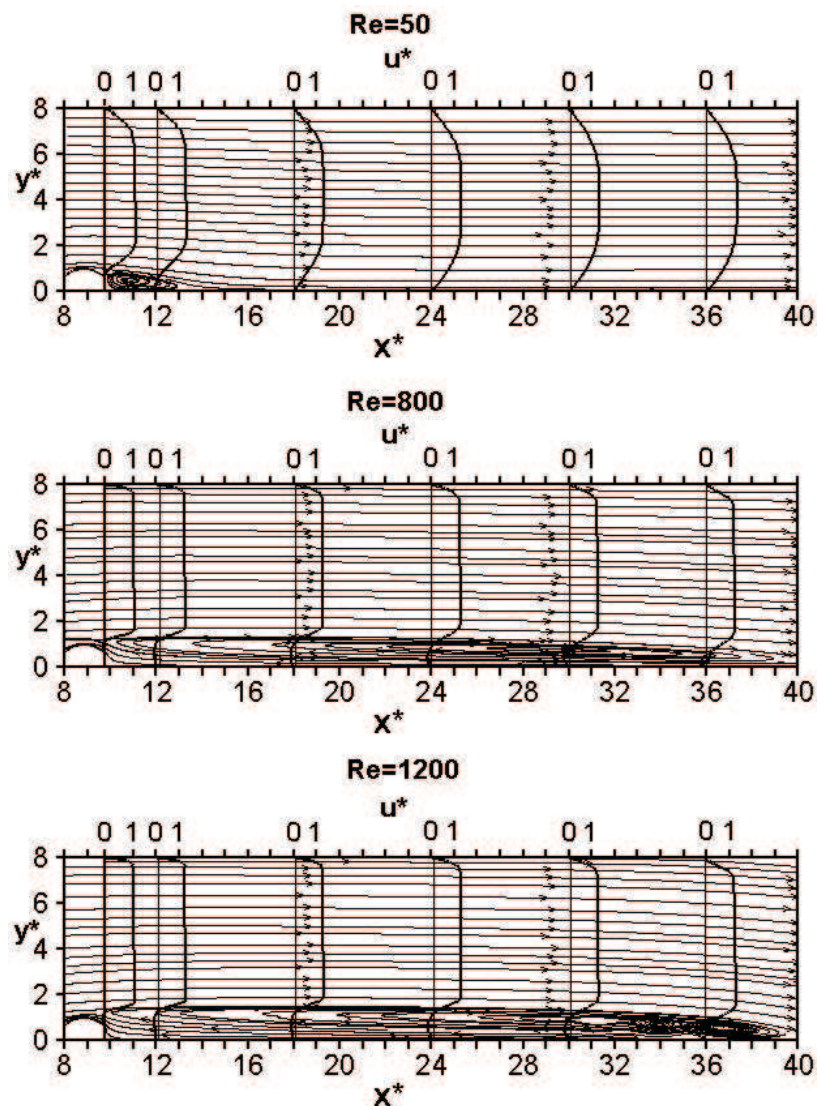
Fig. 4. Computed streamlines and distributions of stream-wise velocity ( $u^*$ ) upstream of the first greenhouse for different Reynolds number ( $50 \leq Re \leq 1200$ ).

Fig. 5. Details of streamlines and distributions of stream-wise velocity ( $u^*$ ) over two successive greenhouses for different Reynolds number ( $50 \leq Re \leq 1200$ ).

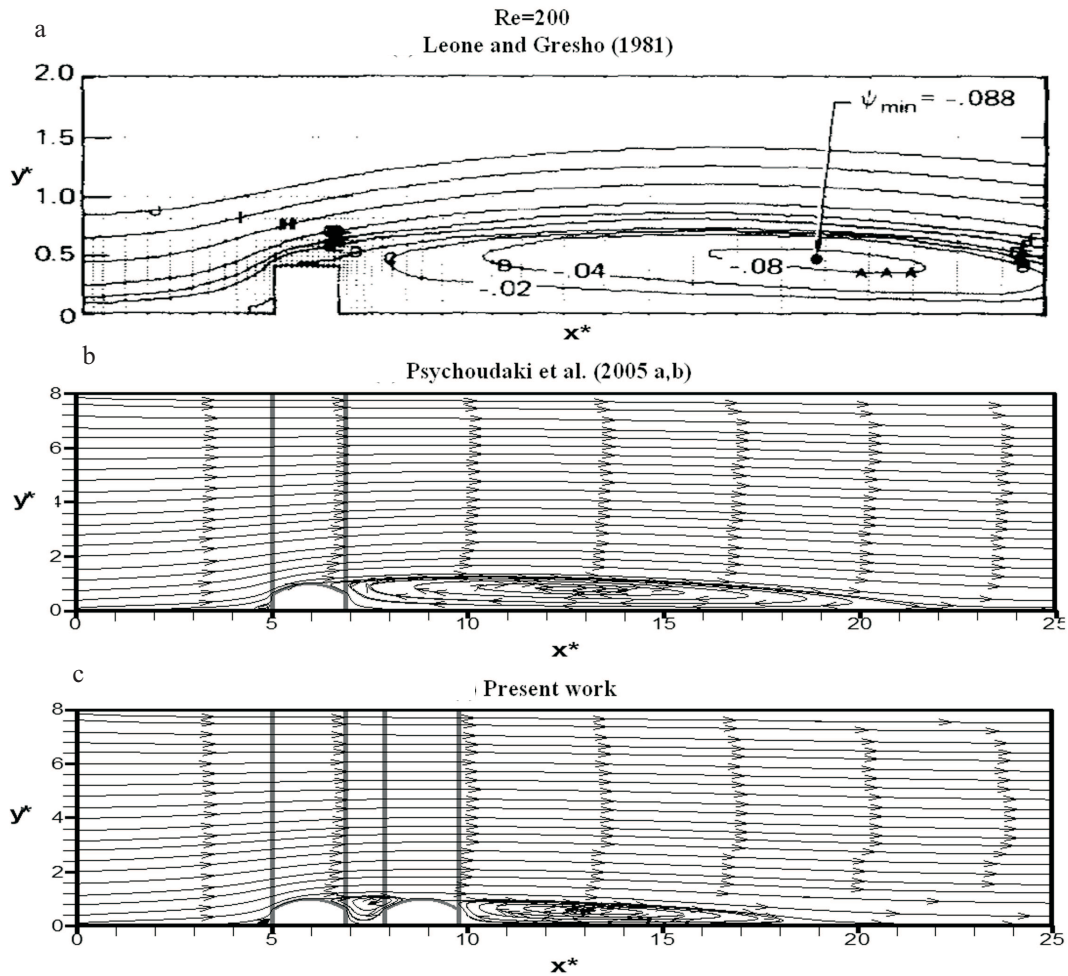
reattached at the half of the second one. Between the greenhouse structures, a single vortex is developed with a negative spin, when  $Re \leq 200$ . When  $Re \geq 400$ , two opposite vortices appear, one negative and one positive. The upper negative rotating flow is united with the rotating flow downstream of the second greenhouse, when  $Re \geq 800$ . The existence of local vortices in the flow can generate lift forces and causes damages to the greenhouses, if the vortex intensity is increased due to an increase of Reynolds number. The indicative distributions of the stream-wise velocity ( $u^*$ ) present constant values outside the boundary layer. At the boundary layer, velocity values are reduced smoothly and in the recirculation area become zero to obtain negative values (reverse air flow) and to become zero again at the wall in accordance with the boundary conditions.

Figure 6 depicts the details of the streamlines downstream of the second greenhouse, for  $50 \leq Re \leq 1200$ . It is clear that the recirculation length is increasing as Reynolds number is increasing. It can be seen that negative stream-wise velocity values are presented in all recirculation regions of flow (Figs 4-6), but higher absolute negative values of stream-wise velocity are observed downstream of the second greenhouse.

Figure 7 presents a qualitative comparison of the streamlines among the present study (case c) and those of Leone and Gresho (1981) in a rectangular construction (case a) and Psychoudaki *et al.* (2005a,b) in a single span tunnel greenhouse (case b), for  $Re = 200$ . The similarities between the recirculation flow regions, upstream and downstream of the structures are obvious for all cases. It must be noted that in



**Fig. 6.** Computed streamlines and distributions of stream-wise velocity ( $u^*$ ) downstream of the second greenhouse for different Reynolds number ( $50 \leq Re \leq 1200$ ).



**Fig. 7.** Qualitative comparison of streamlines for  $Re = 200$ : a – Leone and Gresho (1981), b – Psychoudaki *et al.* (2005 a,b) and c – present work.

all cases, the equations of Navier-Stokes were numerically solved by the finite element method. In cases (a) and (b), it is observed that there is a similarity in the boundary layer separation process over the structure roof, which creates a reverse flow downstream of the structure. On the contrary, in the present study (case c) the separation of the boundary layer begins in the downstream end of the second greenhouse, due to the larger total width of the successive greenhouses. In cases (b) and (c), more detailed streamlines are observed in relation to case (a), due to better boundary conditions and to the choice of a computational domain, which includes a greater number of elements, nodes and unknowns.

The calculated separated and reattachment lengths of the boundary layer, with regard to the Reynolds number are presented in Fig. 8, cases (a) and (b) respectively. In case (a), the variation of the separation length ( $x^*_S$ ) is shown upstream of the first greenhouse. The separation length is increasing as the Reynolds number is increasing. It is also observed that the increase of the separation length is more

intense, when  $10 \leq Re \leq 500$ , while it becomes less intense, when  $600 \leq Re \leq 1\ 200$ . The best fitting equation describing the separate length distribution is a 3rd degree polynomial, with a correlation coefficient value of  $R^2 = 0.9951$  ( $R^2$  approaching to 1). In case (b), the variation of the reattachment length ( $x^{**}_R$ ) is depicted downstream of the second greenhouse, where  $x^{**}_R = 0$  in the downstream base of the second greenhouse. The reattachment length is increasing as the Reynolds number is increasing. The best fitting equation describing the reattachment length distribution is a 2nd degree polynomial, with a correlation coefficient value  $R^2 = 0.9926$  ( $R^2$  approaching to 1).

In order to validate the mathematical code, the calculated results of the present study are compared with other computational and experimental results, regarding to the separation-reattachment lengths of boundary layer. In Fig. 9a, the studies of Fragos *et al.* (1997) and Hong *et al.* (1991), (rectangular obstacles, cases  $y_8$  and  $y_3$ , respectively) and Psychoudaki *et al.* (2005a,b), (single span tunnel greenhouse, case  $y_2$ ) are

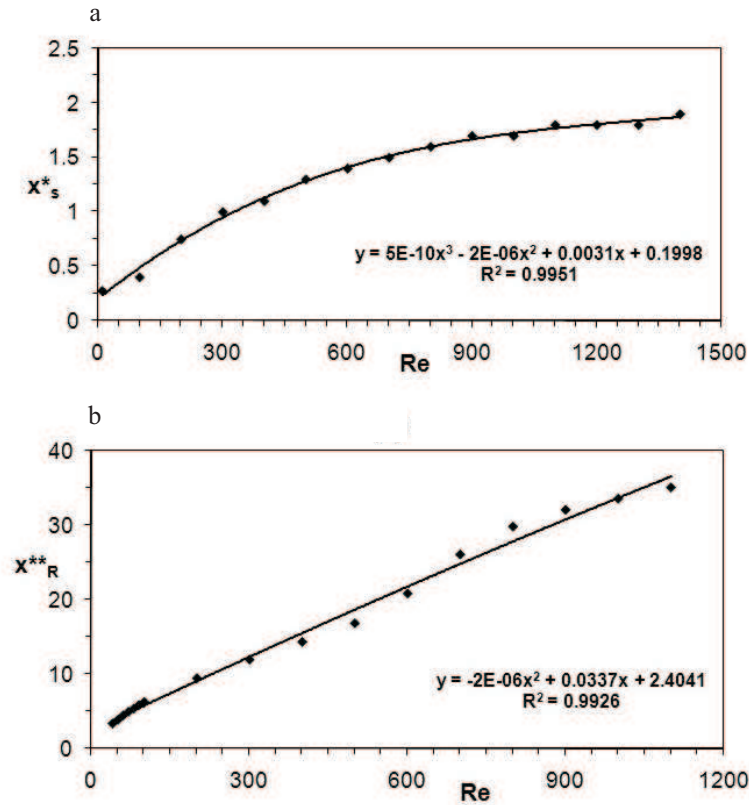


**Fig. 8.** Separation length upstream of the first greenhouse ( $x^*_s$ ) – a, and reattachment length downstream of the second greenhouse ( $x^{**}_R$ ) – b.

compared with the present study (two successive single span tunnel greenhouses, case  $y_1$ ) regarding to the separation length ( $x^*_s$ ). It is observed that the separation length is increasing as the Reynolds number is increasing in all cases. All distributions of the separation length can be expressed by a 3rd degree polynomial with a correlation coefficient from  $R^2=0.9853$  to  $R^2=1$ . Each equation has a different slope depending on the geometry of the structures. It is also observed that the curve of the separation length in case ( $y_2$ ) is almost similar compared with case ( $y_1$ ), for  $0.02 < Re < 760$ . The slight difference is owed to the width of the structures. In the other two cases ( $y_3$  and  $y_8$ ), concerning to rectangular structures, the slope of the curves are steeper. This variation is attributed to the different geometry of these structures (presence of a sharp upstream edge).

In Fig. 9b, experimental data of Acrivos *et al.* (1968), Hong *et al.* (1991), Boum *et al.* (1999), (rectangular obstacles, cases  $y_4$ ,  $y_8$  and  $y_5$ , respectively) and Denham and Patric (1974), Armaly *et al.* (1983), (backward-facing step, cases  $y_7$  and  $y_6$ , respectively), are compared with computational data of Fragos *et al.* (1997), (rectangular obstacle, case  $y_3$ ), Psychoudaki *et al.* (2005a, b), (single span tunnel greenhouse, case  $y_2$ ) and the present study (two successive single span tunnel greenhouses, case  $y_1$ ). It can be seen that the

reattachment length is influenced by the Reynolds number and the geometry of the obstacles or the structures. In particular, the curves of the reattachment length in cases ( $y_3$ ,  $y_4$  and  $y_5$ ), which are rectangular structures or 'bluff bodies' with small width and  $Re < 100$ , coincide and have larger slopes compared to the other cases. The curves in cases ( $y_6$  and  $y_7$ ), (backward-facing step) and the present study for  $Re < 300$ , also coincide but they have much smaller slope than the rectangular structures. Consequently, the sharp edges of the rectangular, flat, horizontal roof result in an increased recirculation length, in contrast to the tunnel roofs with smooth edges (geometry effect). For the same Reynolds number, the reattachment length, in two successive single span tunnel greenhouses case ( $y_1$ ) is smaller compared to that of the single span tunnel greenhouse case ( $y_2$ ), for  $0.02 < Re < 760$ . It should be noticed that the total width of the successive single span tunnel greenhouses is larger than the width of the single span tunnel greenhouse. This result is in good agreement with the conclusion of Hwang *et al.* (1999), reporting that an increase of the structure width reduces the reattachment length, ( $x^{**}_R$ ). The distribution curves of the reattachment length, for all studies, are described by 2nd degree polynomials with a correlation coefficient  $R^2 \approx 0.99$ , approximately.

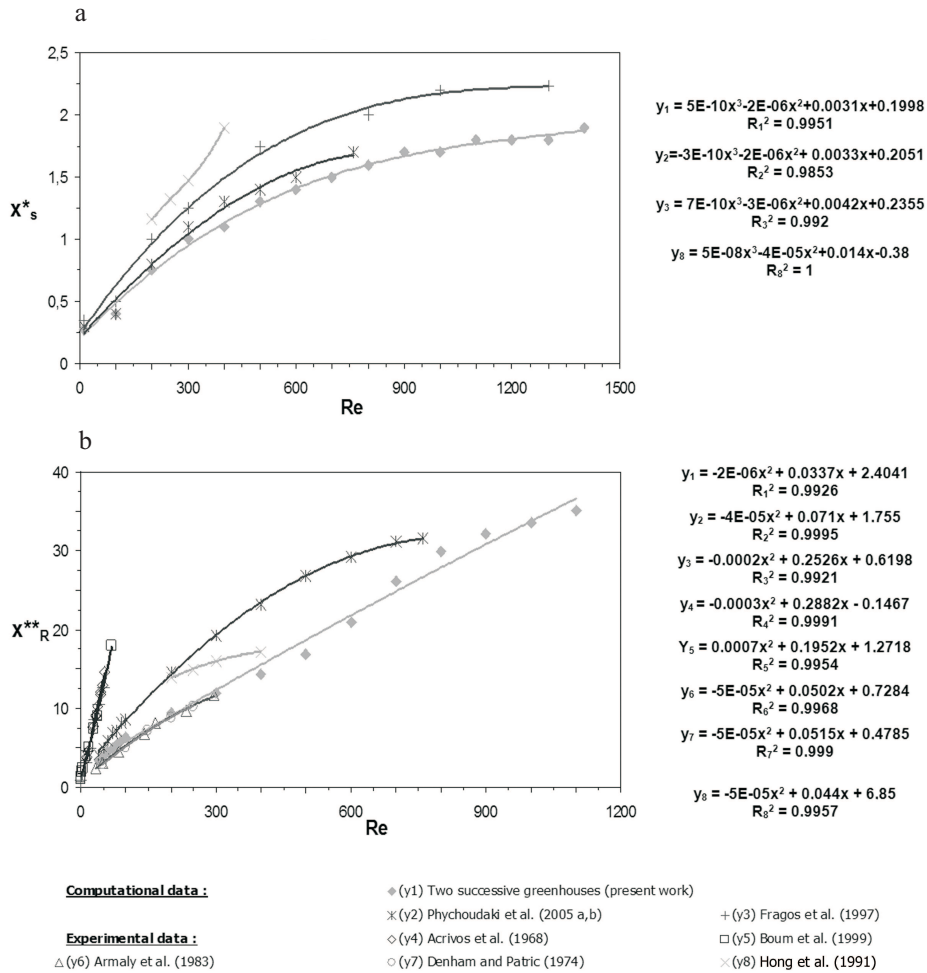


**Fig. 9.** Comparison of the calculated separation (a) and reattachment length (b) of the boundary-layer versus computational and experimental data by other researches.

CONCLUSIONS

1. The distribution of the airflow streamlines, along the computational domain for various Reynolds numbers, shows three recirculation regions of flow (vortices), due to the separation of the boundary layer which is owed to the presence of the greenhouses. These regions are upstream of the first greenhouse, between the greenhouses and downstream of the second greenhouse. The recirculation regions and the vortices distribution are predicted reasonably well by the proposed numerical approach.

2. Negative stream-wise velocity values are presented in each recirculation region of flow. The vortex formation is larger downstream of the second greenhouse. The formation of local flow vortices may generate lift forces which can cause damages to the greenhouses.

3. The separation length of the boundary layer, upstream of the first greenhouse, is increasing as the Reynolds number is increasing. The slope of the separation length

distribution is affected by the greenhouses geometry. The correlation between the separation length and the Reynolds number is described by a 3rd degree polynomial, with correlation coefficient  $R^2 > 0.9951$  ( $R^2$  approaching to 1).

4. The reattachment length of the boundary layer, downstream of the second greenhouse, is directly correlated with the Reynolds number and the greenhouses geometry. By increasing the Reynolds number, an increase of reattachment length is obviously presented, but not proportional, due to the geometry of the greenhouse structures. Also, the length of reattachment is decreasing as the width of the greenhouses is increasing. The correlation between the reattachment length and the Reynolds number is described by a 2nd degree polynomial, with correlation coefficient  $R^2 > 0.9926$  ( $R^2$  approaching to 1).

5. The results of this study compared with computational and experimental results of other researchers confirm that the used mathematical code approximates with accuracy the airflow over two successive greenhouses.

6. The studied numerical procedure combined with the escalating development of computers can be used to predict two or three dimensional, unsteady flow, at different geometries and flow conditions, in the external and internal environment of several agricultural structures.

#### REFENENCES

- Acrivos A., Leal L.G., Snowden D.D., and Pan F., 1968.** Further experiments on steady separated flows past bluff objects. *J. Fluid Mechanics*, 34(1), 25-48.
- Antoniou J. and Bergeles G., 1988.** Development of the reattached flow behind surface-mounted two-dimensional prisms. *J. Fluids Eng.*, 110, 127-133.
- Armaly B.F., Durst F., Pereira J.C.F., and Schonung B., 1983.** Experimental and theoretical investigation of backward-facing step flow. *J. Fluid Mechanics*, 127, 473-496.
- Boum Ngo G.B., Martemianov S., and Alemany A., 1999.** Computational study of laminar flow and mass transfer around a surface-mounted obstacle. *Int. J. Heat Mass Transfer*, 42, 2849-2861.
- Bournet P.-E. and Boulard T., 2010.** Effect of ventilator configuration on the distributed climate of greenhouses: A review of experimental and CFD studies. *Comp. Electronics Agric.*, 74(2), 195-217.
- Denham M.K. and Patrick M.A., 1974.** Laminar flow over a downstream-facing step in a two-dimensional flow channel. *Trans. Inst. Chem. Eng.*, 52, 361-367.
- Erpul G., Gabriels D., and Janssens D., 2000.** Effect of wind on size and energy of small simulated raindrops: a wind tunnel study. *Int. Agrophysics*, 14, 1-7.
- Fragos V.P., Psychoudaki S.P., and Malamataris N.A., 1997.** Computer-aided analysis of flow past a surface-mounted obstacle. *Int. J. Numerical Methods Fluids*, 25, 495-512.
- Fragos V.P., Psychoudaki S.P., and Malamataris N.A., 2007.** Direct simulation of two-dimensional turbulent flow over a surface-mounted obstacle. *Int. J. Numerical Methods Fluids*, 55, 985-1018.
- Gresho P.M. and Sani R.L., 1998.** *Incompressible Flow and The Finite Element Method*. Wiley Press, New York, USA.
- Hong Y.-J., Hsieh S.-S., and Shih H.-J., 1991.** Numerical computation of laminar separation and reattachment of flow over surface mounted ribs. *J. Fluids Eng.*, 113, 190-198.
- Hwang R.R., Chow Y.C., and Peng Y.F., 1999.** Numerical study of turbulent flow over two-dimensional surface-mounted ribs in a channel. *Int. J. Numerical Methods Fluids*, 31, 767-785.
- Leone J.M. and Gresho P.M., 1981.** Finite element simulations of steady, two dimensional, viscous incompressible flow over a step. *J. Computational Physics*, 41, 167-191.
- Macagno E.O. and Hung T.-K., 1967.** Computational and experimental study of a captive annular eddy. *J. Fluid Mechanics*, 28(1), 43-64.
- Malamataris N.A., 1991.** *Computed-aided analysis of flows on moving and unbounded domains: phase-change fronts and liquid leveling*. Ph. D. Thesis, Univ. Michigan, Ann Arbor, MI, USA.
- Molina-Aiz F.D., Fatnassi H., Boulard T., Roy J.C., and Valera D.L., 2010.** Comparison of finite element and finite volume methods for simulation of natural ventilation in greenhouses. *Comp. Electr. Agric.*, 72(2), 69-86.
- Nalbandi H., Seïiedlou S., and Ghassemzadeh H.R., 2010.** Aerodynamic properties of *Turgenia latifolia* seeds and wheat kernels. *Int. Agrophysics*, 24, 57-61.
- Norton T., Sun D.-W., Grant J., Fallon R., and Dodd V., 2007.** Applications of computational fluid dynamics (CFD) in the modelling and design of ventilation systems in the agricultural industry: A review. *Bioresour. Technol.*, 98(12), 2386-2414.
- Owen D.R.J. and Hinton E., 1980.** *Finite Elements in Plasticity: Theory and Practice*. Pineridge Press, Swansea, UK.
- Papanastasiou T.C., Malamataris N., and Ellwood K., 1992.** A new outflow boundary condition. *Int. J. Numerical Methods Fluids*, 14, 587-608.
- Psychoudaki S.P., Laskos V.N., and Fragos V.P., 2005a.** A two-dimension computational investigation of the flow over a wall-mounted parabolic body. *Proc. 3rd IASME/ WSEAS Int. Conf. Fluid Mechanics and Aerodynamics*. August 20-22, Corfu, Greece.
- Psychoudaki S.P., Laskos V.N., and Fragos V.P., 2005b.** Numerical analysis of viscous flow over a mounted parabolic body. *IASME Trans.*, 7(2), 1207-1216.
- Vassiliou N.N., Martzopoulos G.G., and Nikita-Martzoopoulou Ch., 1999.** Air flow pattern outside and inside a double span arch type greenhouse. *Proc. IFAC Workshop Control Applications and Ergonomics in Agriculture*, June 14-17, Athens, Greece.
- Zienkiewicz O.C., Taylor R.L., and Nithiarasu P., 2005.** *The Finite Element Method for Fluid Dynamics*. Butterworth-Heinemann Press, Oxford, UK.